ELSEVIER

Journal of South American Earth Sciences 24 (2007) 25–33

Journal of
South American
Earth Sciences

www.elsevier.com/locate/jsames

Ages and possible provenance of the sediments of the Capim River kaolin, northern Brazil

D.J.L. Sousa [a,b], A.F.D.C. Varajão [a,*], J. Yvon [b], T. Scheller [c], C.A.V. Moura [c]

[a] *DEGEO – Departamento de Geologia, Universidade Federal de Ouro Preto, Ouro Preto, MG, Brazil*
[b] *LEM – Laboratoire Environnement et Minéralurgie/ENSG/INPL, Vandoeuvre lès Nancy, France*
[c] *PARAISO – Laboratório de Geologia Isotópica, Universidade Federal do Pará, Belém, Brazil*

Received 1 February 2005; accepted 1 January 2007

Abstract

Provenance studies carried out on the soft and flint facies of the Capim River kaolin (northern Brazil) trace the possible sources of sediments that host the ore. Pb–Pb evaporation geochronology was applied to four predominant morphologic classes of detrital zircons, and the ages obtained were compared to the main age intervals of the rocks surrounding the Capim kaolin district (CKD). Four major plateau ages (2.15, 2.02, 1.87, and 1.51 Ga) were defined for both soft and flint facies, indicating a common source for the kaolin and provenance from NE and SW. The 2.15 and 2.02 Ga ages correlate with the granitic bodies of the Gurupi region, located NE of the study area. The 1.87 and 1.51 Ga ages show provenance from the Amazon Craton, the former from the southern portion, in the Carajás region, and the latter from the southwestern portion. Although less abundant, Archean (3.18, 2.79, and 2.55 Ga) and Neoproterozoic ages (0.8 and 0.51 Ga) also correlate with the SW and NE provenances, respectively. The first corresponds to the oldest rocks of the Carajás region and the second to the rocks of the Gurupi region, corresponding to the Brasiliano orogeny.

Keywords: Pb–Pb geochronology; Provenance zircon; Capim kaolin; Cametá sub-basin; Northern Brazil

1. Introduction

Brazilian Amazonia contains 10% of the world reserves of kaolin. The major occurrences are found in the Capim River region, northeast of Pará State, known worldwide as the Capim kaolin district (CKD). Due to the high average whiteness index (90 ISO), Capim River kaolin is used exclusively in the paper coating industry and exported to the United States, Europe, and Asia.

The Capim River kaolin occurs in the Ipixuna Formation (Late Cretaceous–Early Tertiary), composed of a soft kaolin (main ore) that grades to a hard (flint) kaolin (Sousa, 2000). The economic importance of the CKD has prompted scientific interest since the 1970s, with studies encompassing both general works on geology and genesis (Krebs and Arantes, 1973; Hurst and Bosio, 1975; Monteiro, 1977; Murray and Partridge, 1981) and specified mineralogical, geochemical, and facies distribution studies (Costa and Moraes, 1992, 1998; Moraes and Costa, 1993; Moraes, 1994; Kotschoubey et al., 1996; Sousa, 2000; Barbosa, 2002; Nascimento, 2002; Santos, 2002; Barbosa et al., 2004). Despite the many studies, controversies still exist regarding the origin and relationships of soft and flint facies—that is, whether their differentiation relates to the contribution of different sediment sources or if it is due to weathering after deposition. This work investigates the possible sources of sediments that form kaolin.

Prior provenance studies of the sediments that constitute the Capim River kaolin were based on paleocurrent measurements and zircon typology analyses. Santos (2002) and Santos and Rossetti (2003) suggest northwestern and south-southwestern provenances, but their data are insufficient to confirm the sediment sources. Nascimento (2002),

* Corresponding author. Tel.: +55 31 35591605; fax: +55 31 35591606.
E-mail address: angelica@degeo.ufop.br (A.F.D.C. Varajão).

0895-9811/$ - see front matter © 2007 Elsevier Ltd. All rights reserved.
doi:10.1016/j.jsames.2007.02.007

using tourmaline and zircon varieties and paleocurrent data, suggests that the sediments come either from the southwest (Amazon Craton) or south (Araguaia belt), with possible contribution from the northeast (Gurupi region).

This research offers new data regarding Eastern Amazonia and uses single zircon direct evaporation geochronology with the Pb–Pb method to access the provenance of the sediments that produced the Capim River ore by correlating ages found in the region. Similar attempts to understand the provenance of the Amazon Craton Proterozoic sedimentary cover have been carried out by Leite and Saes (2003) using the same method and Rino et al. (2004), who apply sensitive high resolution ion microprobe (SHRIMP) methods to zircons from the Amazon River mouth. Sousa et al. (2002) offer the first attempts to correlate the Capim soft kaolin zircons with the granitoid bodies cropping out in NE Pará and use Pb–Pb geochronology. This article presents a complete study that involves many samples and represents the entire succession.

2. Geological setting

The CKD is located NE of Pará State, northern Brazil (Fig. 1). It belongs to the Cametá sub-basin, at the eastern margin of the Marajó Basin (Galvão, 1991; Villegas, 1994; Costa et al., 2002), and originated from a graben system associated with the opening of the equatorial Atlantic Ocean in the Early Cretaceous. Borges et al. (1997) apply the name Capim River Basin to this triangular graben whose depocenter is filled with the Ipixuna Formation (Francisco et al., 1971), composed of kaolin-bearing sandy sediments that grade upward into pelitic sediments. Francisco et al. (1971) interpret deposition in a fluvial-lacustrine environment, possibly of Early Tertiary age, whereas Borges et al. (1997) suggest a fluvial to transitional-marine environment, and Santos (2002) considers a fluvial and estuarine environment of Upper Cretaceous–Lower Tertiary age for the Ipixuna Formation.

Mineralogic studies (Moraes, 1994; Kotschoubey et al., 1996; Sousa et al., 1999; Sousa, 2000; Barbosa, 2002; Barbosa et al., 2004) define the Capim River kaolin as composed of soft kaolin that grades upward into flint. It is mainly composed of kaolinite and quartz with subordinate hematite, goethite, zircon, rutile, anatase, tourmaline, staurolite, kyanite, muscovite, topaz, and minerals of the crandallite group, in proportions lower than 5%.

The CKD (Fig. 1) is limited to the northeast by Proterozoic granitoid bodies from the Gurupi region, to the northwest by the Guiana Craton, and to the southwest by the Amazon Craton. Its major expression is in the Carajás region to the south, with the oldest rocks of the region.

The first geochronologic studies (Hurley et al., 1967; Almaraz and Cordani, 1969; Wanderley Filho, 1980; Villas, 1982) were based on Rb–Sr and K–Ar methods and allowed recognition of two age domains for the Gurupi region: Paleoproterozoic (~2.0 Ga) and Neoproterozoic (~1.0–0.5 Ga). However, more recent works (Palheta, 2001; Klein and Moura, 2001a,b, 2003; Moura et al., 2003), based on Pb–Pb zircon geochronology, show that most rock units (Table 1), composed of granites and gneisses, formed between 2.2 and 2.0 Ga. Only two bodies, the Boca Nova nepheline syenite and the Ney Peixoto granite (Table 1), reveal Neoproterozoic crystallization ages (~0.72 and 0.55 Ga, respectively).

The eastern portion of the Guianas Craton is composed of Archean tonalitic gneisses, migmatites and granulites (3.1–2.6 Ga), greenstone belts, Paleoproterozoic granitoids and orthogneisses (2.26 Ga), and Paleoproterozoic felsic (1.76 Ga) and alkaline (1.68 Ga) intrusions (Avelar, 2002).

The southwestern region of the Amazon Craton (Table 1) includes granite-gneisses and granitoids, with ages ranging from 1.8 to 1.55 Ga (Tassinari and Macambira, 1999), and a metamorphic province, representing the reworking of older continental crust, with ages from 1.5 to 1.37 Ga (Teixeira et al., 1989; Cordani et al., 2000; Tassinari et al., 2000). The south includes the Carajás region, where geochronologic studies (Teixeira et al., 1989, 2002; Machado et al., 1988, 1991; Macambira and Lafon, 1995; Tassinari and Macambira, 1999; Tassinari et al., 2000), recovered from granitoid bodies and gneisses, indicate ages of 3.0–1.9 Ga. Furthermore, the intrusion of granitoids of the Araguaia belt, related to the Brasiliano orogenic event (0.7–0.4 Ga), suggests ages ranging from 0.583 ± 0.039 Ga (Moura and Gaudette, 1993) to 0.510 ± 0.015 Ga (Barradas et al., 1992).

3. Methods

Representative samples of both soft and flint kaolin were crushed in an agate mortar, followed by heavy minerals concentration by panning. The fine and very fine sand fractions of heavy minerals were concentrated by sieving, followed by dense liquid separation with bromoform. Less magnetic zircons were concentrated using a Frantz Isodynamic magnetic separator, with a 1.5 Å current, 20° forward slope, and side slopes varying from 0° to 5°. To avoid U–Pb fractions from metamictic portions, mineral intergrowths, fractures, incrustations at the rims of crystals, or significant inclusions, the clearest, most transparent, and translucent zircon crystals were handpicked under the stereomicroscope.

Due to the diversity of shapes, the 61 zircon crystals selected (31 from the soft and 30 from the flint kaolin) are grouped into four morphologic types (Fig. 2). Type I is characterized by long, euhedral crystals (length/width > 5), implying that the crystals did not undergo much transport and that the source rock was close to the site of deposition. Type II zircons are composed of intermediate, subhedral to subrounded crystals ($3 \leqslant L/W < 5$) that suggest some transport that caused wearing of the crystal corners. Type III is characterized by short euhedral crystals ($L/W < 3$) with little or no evidence of transport. Type IV is composed of ovoid to spherical zircons, indicating much transport or a history of sediment recycling.

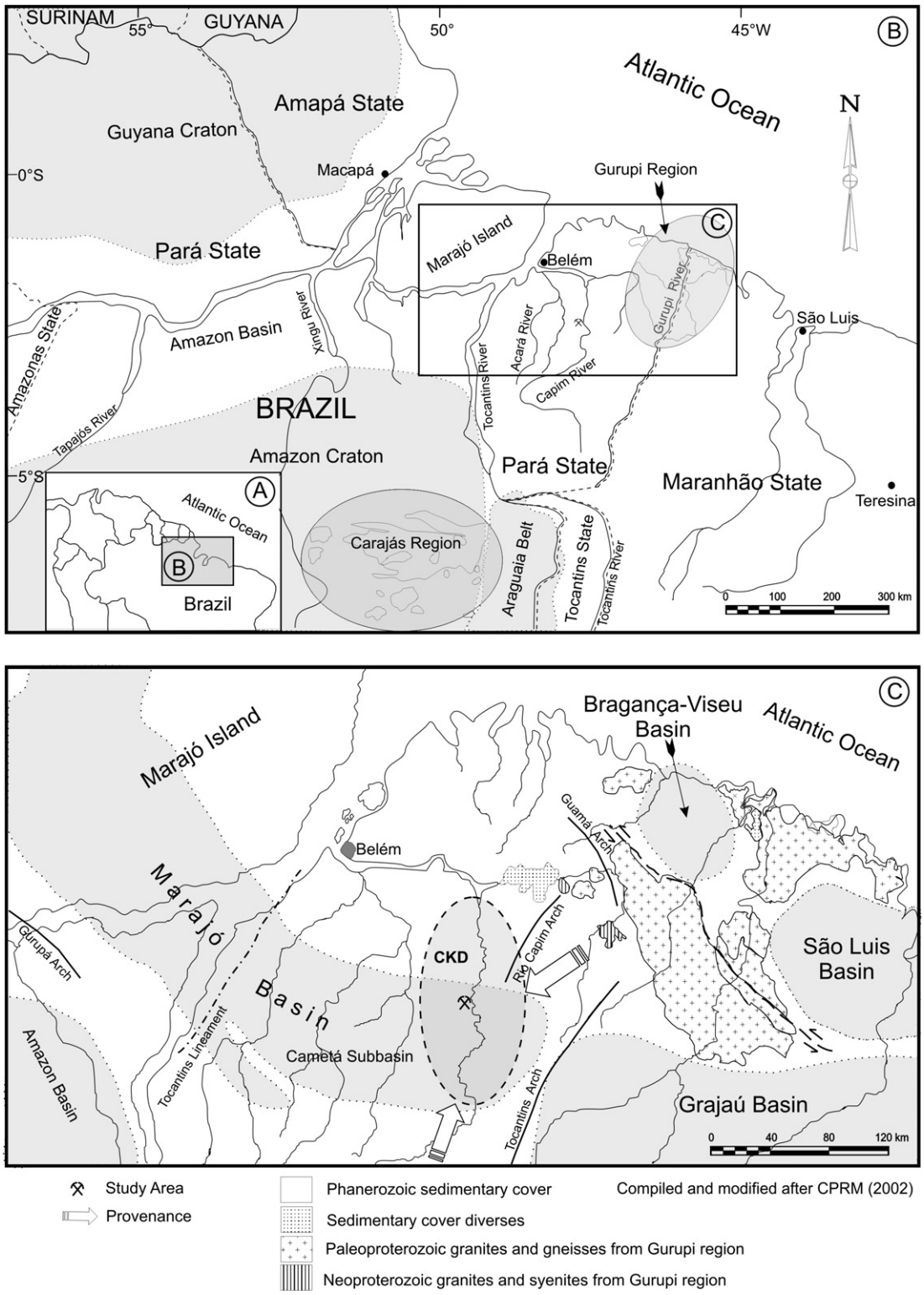

Fig. 1. Location map of the study area. The arrows indicate the possible zircon provenance areas in the CKD, based on the age of the adjacent bodies. See above-mentioned references for further information.

The Pb–Pb isotopic analyses using single zircon evaporation were carried out at the Isotopic Geology Laboratory of the Federal University of Pará (Pará-Iso) with a Finnigan MAT 262 mass spectrometer. The method (Gaudette et al., 1998) consists of determining the $^{207}Pb/^{206}Pb$ apparent age of a zircon crystal using the double-filament technique (Kober, 1986, 1987). The apparent age is interpreted as the age of crystallization of igneous zircons, whereas minimum age refers to metamorphic ones. The ages obtained by Pb–Pb evaporation have the advantage

Table 1
Geochronologic data of the rocks surrounding the Capim Kaolin District (CKD)

Region	Unity/rock	Ages (Ga)	References
Gurupi Region	Tromai suite – granitoids	2.165–2.148	Klein and Moura (2001a)
	Gurupi group – gneiss, schist	2.16–2.148	Klein and Moura (2001a)
	Cantão – granitoids	2.159	Palheta (2001)
	Maracaçumé complex – gneiss	2.135	Klein and Moura (2003)
	Tracuateua suite – granite	2.09	Palheta (2001)
	Jonasa – granitoids		Palheta (2001)
	Japiim – granitoids	2.08	Palheta (2001)
	Ourem – granitoids	2.01	Palheta (2001)
	Boca Nova syenite suite	0.72	Villas (1982)
	Ney Peixoto – granite	0.55	Palheta (2001)
Guianas Craton	Tonalitic gneiss, migmatite, granulite	3.1–2.6	Avelar (2002)
	Greenstone belts, granitoids, orthogneiss	2.26	
	Felsic intrusion	1.76	
	Alkaline intrusions	1.68	
Amazon Craton			
Southwestern	Rio Negro-Juruena province – granite-gneiss	1.8–1.55	Tassinari and Macambira (1999) Teixeira et al. (1989)
	Rondonian-San Ignácio province – gneiss	1.5–1.37	Cordani et al. (2000) Tassinari et al. (2000)
South (Carajás region)	Granites, gneiss	3.0 –1.9	Teixeira et al. (2002, 1989) Machado et al. (1991, 1988) Macambira and Lafon (1995) Tassinari and Macambira (1999) Tassinari et al. (2000)
Araguaia belt	Granitoid intrusion	0.583 0.510	Moura and Gaudette (1993) Barradas et al. (1992)

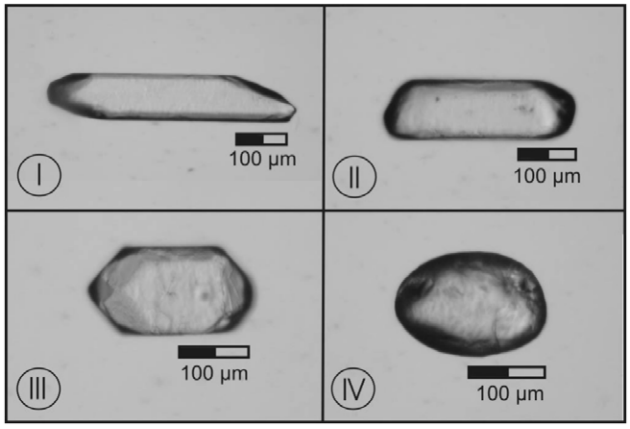

Fig. 2. Morphologic classification of CKD zircon crystals. Type I: long, euhedral crystals; type II: intermediate, subhedral to subrounded crystals; type III: short, euhedral crystals; type IV: oval to rounded crystals.

of being simple and fast compared with the K–Ar, Rb–Sr, and U–Pb methods (Gaudette et al., 1998), because the lack of chemical treatment avoids the risk of contamination. It also is relatively cheap compared with the SHRIMP method. However, this method does not allow for estimations of the degree of data concordance, because the obtained ages are considered minimum ages.

Isotopic analysis by Pb–Pb evaporation consists of mounting the zircon crystals on a rhenium filament parallel to the ionization filament of the thermal ionization mass spectrometer. The evaporation filament heats the zircon crystal, and the ionization filament thermally ionizes Pb for mass spectrometric analysis. The analysis measures the ^{204}Pb, ^{206}Pb, ^{207}Pb, and ^{208}Pb isotopes, and the age is determined as the weighted average of the values corresponding to $^{207}Pb/^{206}Pb$ ratio blocks. The results are presented with 2σ standard deviations.

The data treatment to obtain the initial Pb composition is based on Stacey and Kramers (1975), corrected according to Gaudette et al. (1998). This correction considers a limit value of 0.0004 for the $^{204}Pb/^{206}Pb$ ratio, directly related to contamination or initial Pb; values higher than 0.0004 are discarded.

To obtain the intervals or plateaus of zircon ages, a statistical treatment (Klein and Moura, 2001a,b) based on the ages obtained at higher temperatures is used, because the Pb analyzed came from zircon crystal cells and is more representative of the age of crystallization.

The data obtained provide a correlation with the published minimum ages of the bodies of the region.

4. Results

The selected zircon crystals are colorless to light brown and light pink. Type II zircons predominate at 39%, followed by type III with 32%, type IV with 17%, and type I with 12%.

The results of Pb isotopic analysis of 31 zircon crystals from soft kaolin and 30 zircon crystals from flint kaolin

Table 2
Analytical results for zircons from soft (KS) and flint (KF) kaolin

Kaolin	Type	Zircons	Ev. Temp.[a] (°C)	Util./Total Ratios[b]	$^{204}Pb/^{206}Pb \pm 2\sigma$	$(^{207}Pb/^{206}Pb)c^{c} \pm 2\sigma$	Age (Ma) $\pm 2\sigma$
Soft	Type I	KS-I/1	1500	88/88	0.000042 ± 5	0.13303 ± 29	2139 ± 4
		KS-I/2	1500	90/90	0.000176 ± 27	0.09411 ± 37	1511 ± 7
		KS-I/3	1500	82/82	0.000065 ± 18	0.09495 ± 17	1527 ± 3
		KS-I/4	1550	90/90	0.000007 ± 3	0.13965 ± 21	2223 ± 3
		KS-I/5	1550	88/88	0.000009 ± 3	0.12184 ± 29	1984 ± 4
		KS-I/6	1500	88/88	0.000021 ± 4	0.13434 ± 21	2156 ± 3
		KS-I/7	1450	86/86	0.000081 ± 5	0.09127 ± 24	1452 ± 5
		KS-I/8	1500	84/84	0.000085 ± 8	0.13368 ± 38	2147 ± 5
	Type II	KS-II/9	1500	30/30	0.000020 ± 21	0.17143 ± 110	2572 ± 11
		KS-II/10	1550	84/84	0.000034 ± 4	0.13291 ± 20	2137 ± 3
		KS-II/11	1500	86/86	0.000032 ± 4	0.13380 ± 22	2149 ± 3
		KS-II/12	1550	86/86	0.000215 ± 19	0.11188 ± 53	1830 ± 9
		KS-II/13	1500	18/90	0.000398 ± 32	0.17416 ± 63	2598 ± 6
		KS-II/14	1500	86/86	0.000056 ± 7	0.13307 ± 23	2139 ± 3
		KS-II/15	1500	82/82	0.000009 ± 3	0.13401 ± 42	2151 ± 5
		KS-II/16	1500	18/52	0.000388 ± 44	0.11542 ± 83	1887 ± 13
	Type III	KS-III/17	1450	36/36	0.000080 ± 51	0.12552 ± 105	2036 ± 15
		KS-III/18	1500	90/90	0.000197 ± 12	0.11595 ± 43	1895 ± 7
		KS-III/19	1500	86/86	0.000012 ± 9	0.12851 ± 24	2078 ± 3
		KS-III/20	1500	84/84	0.000000 ± 0	0.11574 ± 48	1892 ± 7
		KS-III/22	1500	84/84	0.000085 ± 7	0.11500 ± 20	1880 ± 3
		KS-III/23	1450	50/50	0.000021 ± 8	0.13434 ± 48	2156 ± 6
		KS-III/24	1500	86/86	0.000214 ± 45	0.13008 ± 71	2099 ± 10
	Type IV	KS-IV/25	1550	18/52	0.000222 ± 24	0.16173 ± 70	2474 ± 7
		KS-IV/26	1450	86/86	0.000150 ± 19	0.13067 ± 24	2107 ± 3
		KS-IV/27	1500	34/34	0.000191 ± 39	0.25028 ± 145	3187 ± 9
		KS-IV/29	1500	90/90	0.000201 ± 30	0.13115 ± 51	2114 ± 7
		KS-IV/30	1500	36/36	0.000076 ± 17	0.11570 ± 42	1891 ± 7
		KSIV/31	1450	36/36	0.000027 ± 3	0.11414 ± 32	1867 ± 5
		KS-IV/32	1500	86/86	0.000116 ± 11	0.05876 ± 16	558 ± 6
Flint	Type I	KF-I/1	1500	26/26	0.000049 ± 9	0.11447 ± 37	1872 ± 6
		KF-I/2	1500	32/32	0.000254 ± 11	0.09335 ± 99	1495 ± 20
		KF-I/3	1500	20/20	0.000110 ± 10	0.09453 ± 91	1519 ± 18
		KF-I/4	1500	8/8	0.000166 ± 10	0.09301 ± 380	1488 ± 77
		KF-I/5	1500	16/16	0.000086 ± 75	0.11604 ± 140	1896 ± 22
		KF-I/6	1450	12/12	0.000074 ± 5	0.11257 ± 25	1842 ± 4
		KF-I/7	1450	6/6	0.000000 ± 0	0.09490 ± 70	1526 ± 14
		KF-I/8	1550	12/12	0.000023 ± 7	0.09489 ± 19	1526 ± 4
		KF-I/9	1550	8/8	0.000000 ± 0	0.12296 ± 30	2000 ± 4
		KF-I/10	1500	16/16	0.000019 ± 4	0.11459 ± 29	1874 ± 5
		KF-I/11	1500	24/24	0.000289 ± 6	0.09246 ± 55	1477 ± 11
		KF-I/12	1450	6/6	0.000099 ± 12	0.09479 ± 96	1524 ± 19
	Type II	KF-II/13	1500	24/24	0.000225 ± 16	0.13522 ± 44	2167 ± 6
		KF-II/14	1450	8/22	0.000229 ± 24	0.13225 ± 49	2128 ± 7
		KF-II/15	1500	16/16	0.000090 ± 8	0.11087 ± 63	1814 ± 10
		KF-II/16	1500	16/16	0.000129 ± 22	0.11164 ± 60	1826 ± 10
		KF-II/17	1500	22/22	0.000331 ± 8	0.05762 ± 61	516 ± 23
		KF-II/18	1500	4/4	0.000000 ± 0	0.06588 ± 48	803 ± 15
		KF-II/19	1550	4/4	0.000038 ± 24	0.13408 ± 47	2152 ± 6
		KF-II/20	1550	16/16	0.000051 ± 6	0.11454 ± 55	1873 ± 9
	Type III	KF-III/21	1500	16/16	0.000221 ± 9	0.12312 ± 48	2002 ± 7
		KF-III/22	1550	18/18	0.000033 ± 16	0.13497 ± 87	2164 ± 11
		KF-III/23	1500	16/16	0.000117 ± 2	0.13310 ± 56	2140 ± 7
		KF-III/24	1500	20/20	0.000022 ± 8	0.13206 ± 28	2126 ± 4
		KF-III/26	1500	14/14	0.000021 ± 19	0.12272 ± 37	1996 ± 5
		KF-III/27	1500	24/24	0.000159 ± 83	0.13298 ± 87	2138 ± 11
	Type IV	KF-IV/28	1550	14/14	0.000008 ± 10	0.12863 ± 58	2080 ± 8
		KF-IV/29	1500	16/16	0.000255 ± 21	0.10593 ± 77	1731 ± 13
		KF-IV/30	1550	24/24	0.000019 ± 7	0.19570 ± 36	2791 ± 3
		KF-IV/31	1500	16/16	0.000000 ± 0	0.06079 ± 36	632 ± 13
		KF-IV/32	1550	20/20	0.000037 ± 8	0.13020 ± 171	2101 ± 23

Zircon types: I, II, III, and IV.
[a] Evaporation temperature stage.
[b] Utilized/total rations.
[c] Corrected rations of common Pb.

appear in Table 2, which shows the evaporation temperature values, ratios used to calculate the apparent ages, $^{204}Pb/^{206}Pb$ and $^{207}Pb/^{206}Pb$ ratios, and ages, grouped according to the four morphologic types.

The statistical analysis of the 31 soft kaolin zircons (Fig. 3A) indicates six age plateaus: 3.187 ± 0.009 Ga (1 zircon), 2.552 ± 0.064 Ga (3 zircons), 2.146 ± 0.023 Ga (15 zircons), 1.881 ± 0.008 Ga (7 zircons), 1.499 ± 0.035 Ga (4 zircons), and 562 ± 0.011 Ga (1 zircon). The three age plateaus of 2.146 ± 0.023 Ga, 1.881 ± 0.008 Ga, and 1.499 ± 0.035 Ga represent 90% of the total selected samples. The age 2.146 ± 0.023 Ga is the most representative; it includes the highest number of zircons. It is followed by the age plateaus of 1.881 ± 0.008 Ga and 1.499 ± 0.035 Ga.

Regarding the ages of each morphological zircon type from the soft kaolin, for type I zircons, the representative intervals are 2.146 ± 0.023 Ga (4 zircons), 1.984 ± 0.004 Ga (1 zircon), and 1.499 ± 0.035 Ga (3 zircons). For type II zircons, the age groups are 2.552 ± 0.064 Ga (2 zircons), 2.146 ± 0.023 Ga (4 zircons), and 1.881 ± 0.008 Ga (2 zircons). Type III zircons reveal ages of 2.146 ± 0.023 Ga (4 zircons) and 1.881 ± 0.003 Ga (3 zircons). Finally, for type IV, the ages are 3.187 ± 0.009 Ga (1 zircon), 2.552 ± 0.064 Ga (1 zircon), 2.146 ± 0.023 Ga (2 zircons), 1.881 ± 0.008 Ga (2 zircons), and 0.562 ± 0.011 Ga (1 zircon).

Therefore, grouping by type shows that the most representative age interval of 2.146 ± 0.023 Ga for the soft kaolin is represented by all four zircon types. The second most frequent age, 1.881 ± 0.008 Ga, is represented by types II, III, and IV. The 1.499 ± 0.035 Ga age is represented by type I and 2.552 ± 0.064 Ga by types II and IV. The extreme values of 3.187 ± 0.009 Ga and 0.562 ± 0.011 Ga are represented only by type IV.

The statistical analysis of 30 flint kaolin zircons (Fig. 3B) indicates eight age intervals: 2.791 ± 0.003 Ga

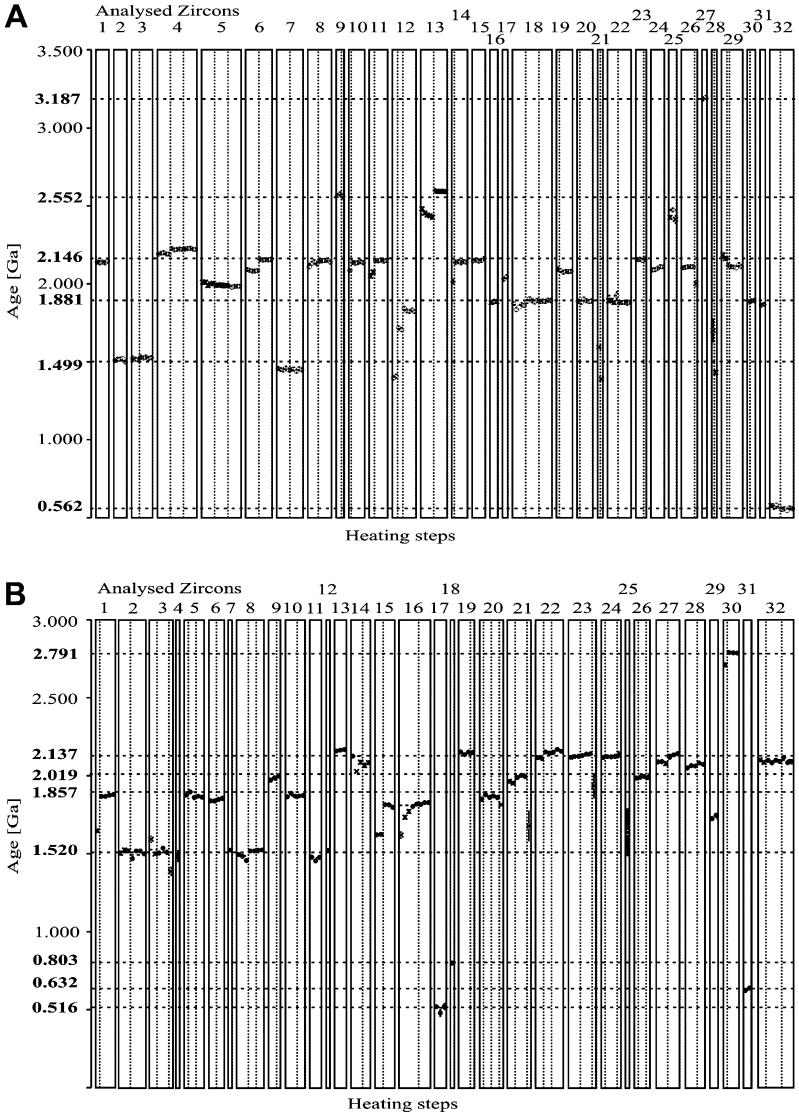

Fig. 3. Diagram of distribution of age plateaus for the soft (A) and flint (B) kaolin. The statistic calculation of the apparent ages, adjusted to two sigma, includes only the stages that correspond to the highest ages.

(1 zircon), 2.137 ± 0.009 Ga (7 zircons), 1.857 ± 0.014 Ga (8 zircons), 1.520 ± 0.009 Ga (7 zircons), 2.019 ± 0.027 Ga (5 zircons), 0.803 ± 0.015 Ga (1 zircon), 0.632 ± 0.013 Ga (1 zircon), and 0.516 ± 0.023 Ga (1 zircon). Four age intervals—2.137 ± 0.009 Ga, 2.019 ± 0.027 Ga, 1.857 ± 0.014 Ga, and 1.520 ± 0.009 Ga—represent 87% of the selected samples.

With regard to the ages of each morphological zircon type from the flint kaolin, for type I zircons, the representative intervals are 2.019 ± 0.027 Ga (1 zircon), 1.857 ± 0.014 Ga (4 zircons), and 1.520 ± 0.009 Ga (7 zircons). For type II zircons, the age groups are 2.137 ± 0.009 Ga (3 zircons), 1.857 ± 0.014 Ga (3 zircons), 0.803 ± 0.015 Ga (1 zircon), and 0.516 ± 0.023 Ga (1 zircon). Type III zircons yield 2.137 ± 0.009 Ga (4 zircons) and 2.019 ± 0.027 Ga (2 zircons). Type IV zircons are represented by 2.791 ± 0.003 Ga (1 zircon), 2.019 ± 0.027 Ga (2 zircons), 1.857 ± 0.014 Ga (1 zircon), and 0.632 ± 0.013 Ga (1 zircon).

Grouping by type provides the same result obtained for the flint kaolin; the most representative age intervals contain the most diversified morphologic types. Thus, 2.137 ± 0.009 Ga is represented by types II and III; 2.019 ± 0.027 Ga by types I, III, and IV; and 1.857 ± 0.014 Ga by types I, II, and IV. The 1.520 ± 0.009 Ga interval is well represented by type I zircons. For the zircons of Brasiliano ages, two crystals represent type II (0.516 ± 0.023 and 0.803 ± 0.015 Ga) and one represents type IV (0.632 ± 0.013 Ga). The 2.791 ± 0.003 Ga zircon is type IV.

Histograms with class intervals of 100 Ma (Fig. 4) show that of the 61 zircons from both soft and flint kaolins, 52, representing 85% of the total, fall in the four most representative age intervals, which include the largest number of morphologic types: 2.152 ± 0.016 Ga (21 zircons), 2.019 ± 0.027 Ga (5 zircons), 1.870 ± 0.010 Ga (16 zircons), and 1.508 ± 0.020 Ga (11 zircons). The remaining 15% are distributed within the age intervals of the isolated zircons: 3.187 ± 0.009 Ga, 2.791 ± 0.003 Ga, 2.552 ± 0.064 Ga, 0.803 ± 0.015 Ga, 0.632 ± 0.013 Ga, and 0.516 ± 0.023 Ga.

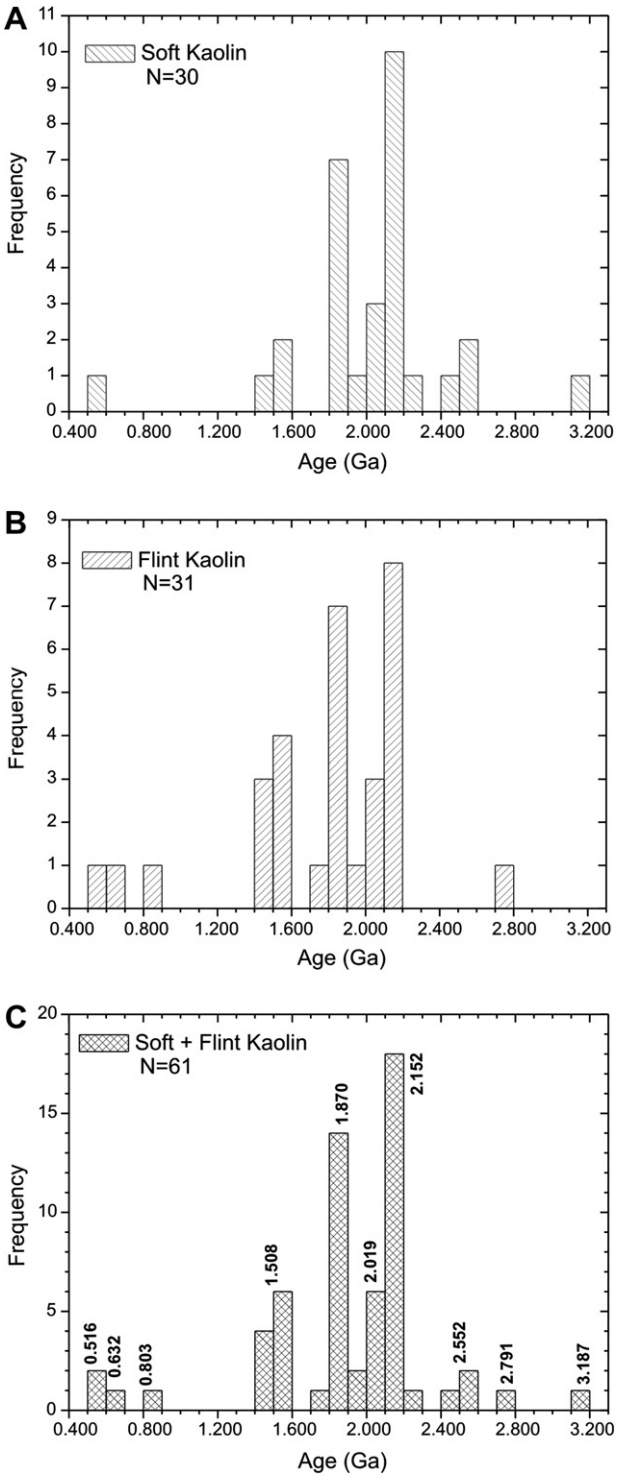

Fig. 4. Frequency histogram of zircon ages for soft, flint, and the combination.

5. Discussion and conclusion

The four major zircon age plateaus of the CKD are observed in both soft and flint kaolin facies, which indicates a common source for the sediments that generated the Capim River kaolin.

Among the four age plateaus, 2.15 and 2.02 Ga are the best defined age intervals for the Capim kaolin zircons, because they correspond to the intervals with the highest amount of zircons and four morphologic types. This Paleoproterozoic plateau is also the most frequently found in the Amazon River mouth zircons (Rino et al., 2004). It correlates with the Gurupi granitoids, located approximately 100 km northeast of the study area, related to the Transamazonian orogenic event and its corresponding Eburnean event in Western Africa. The correlation of these two age plateaus with the Guianas Craton rocks of 2.2 Ga (Avelar, 2002) cannot be ruled out, though the age values obtained in this study do not agree perfectly with the age values of the Guianas Craton.

Ages around 1.87 Ga can be correlated with those of the granites of the Carajás region, south of the Amazon Craton (Machado et al., 1991; Macambira and Lafon, 1995; Cordani et al., 2000; Tassinari et al., 2000; Teixeira et al., 2002). In the same way, apparent Mesoarchean and Neoarchean ages of 3.18 and 2.79 Ga, represented by soft and flint kaolin type IV zircons, provide good correlations with the oldest ages of rocks of the Carajás region. The same is valid for the Neoarchean age of 2.55 Ga, calculated using 3 soft kaolin zircons, which can be correlated with granites from Carajás region. This correlation considers that the study area is located in the eastern margin of the Cametá sub-basin and that, according to Carvajal et al. (1989), one of the principal vectors of fluvial sediment transport of this sub-basin comes from the southern portion. Paleocurrent data (Nascimento, 2002; Santos and Rossetti, 2003) corroborate this hypothesis. The supposition of a contribution of Archean rocks of the Guianas Craton, as suggested by Santos (2002), cannot be supported because the age values obtained in this study do not align with the age values of this region.

The ages of 1.5 Ga do not correlate exactly with the records found or described for rocks surrounding the study area, which suggests that the zircons resulted from either reworking of sediments from unknown sources or were transported for long distances. However, when compared with the data obtained for the Amazon Craton (Tassinari and Macambira, 1999), this age interval appears typical of the southwestern side of the craton (Cordani et al., 2000; Tassinari et al., 2000). For the Amazon River mouth zircons, Rino et al. (2004) report ages that can be correlated with the southwestern side of the craton (Table 1). However, because this age has been represented by a morphology suggesting minimal transport (type I), and the correlated source is located far from the studied area, statistical sampling error should be considered and exclude certain (colored, rimmed, fractured) zircons. The probable age of some of these excluded zircon crystals may mask the representative morphology of the interval age or even complete an age interval.

Zircon ages in the Neoproterozoic–Early Cambrian range (0.80 and 0.51 Ga) correspond to the thermal-tectonic Brasiliano event, recorded in the Gurupi region (Boca Nova alkaline suite gneisses, Ney Peixoto granite; Hurley et al., 1967; Villas, 1982; Palheta, 2001).

Therefore, the results of this study identify two main sediment sources (Fig. 1C), corroborated by previous paleocurrent measurements (Nascimento, 2002; Santos and Rossetti, 2003): one located to the northeast, in the Gurupi region, and another located in the southwestern and southern (Carajás region) portion of the Amazon Craton.

Acknowledgements

The authors thank CNPq and CAPES/COFECUB for financial support and Para-Iso (UFPa Isotopic Geology Laboratory) for geochronologic analyses. The authors are grateful to two reviewers, D. Barbeau and J.A. Dexheimer Leite, for their significant contributions to improving the manuscript.

References

Almaraz, J.S.U., Cordani, U.G., 1969. Delimitação entre as províncias geocronológicas pré-cambrianas ao longo do Rio Gurupi. In: 23 Congresso Brasileiro de Geologia, SBG, Salvador, Boletim Especial.

Avelar, V.G., 2002. Geocronologia Pb–Pb em zircão e Sm–Nd rocha total da porção centro-norte do Estado do Amapá-Brasil: Implicações para a evolução geodinâmica do setor oriental do Escudo das Guianas, 213 p. (PhD Thesis, Centro de Geociências, Universidade Federal do Pará, Belém).

Barbosa, E.M., 2002. Evolution du kaolin supergene de la Riviere Capim (Nord Est du Pará – Brésil). Relations entre les caractéristiques minéralogiques, cristallochimiques et les propriétés industrielles, 165 p. (PhD Thesis, Laboratoire Environnement et Minéralurgie, INPL, Nancy).

Barbosa, E., Varajão, A.F.D.C., Yvon, J., Allard, T., Balan, E., Morin, G., Abdelmouma, M., 2004. Iron EPR logging as a tool for stratigraphic determinations: application to Rio Capim kaolin deposit (Brazil). Journal of Mining and Metallurgy 40, 1–9.

Barradas, J.A., Lafon, J.M., Kotschoubey, B., 1992. Geocronologia Pb–Pb e Rb–Sr da região de Monte do Carmo-Porto Nacional, TO. Novos resultados. In: Anais 37 Congresso Brasileiro de Geologia, SBG, São Paulo 6, pp. 182–183.

Borges, M.S., Costa, J.B.S., Hasui, Y., Fernandes, J.M.G., Bemerguy, R.L., 1997. Instalação e inversão da Bacia do Capim. In: 6 SNET, SBG/CPGQ, Brasília, DF. Boletim de Resumos Expandidos, pp. 134–135.

Carvajal, D.A., Dorman, J.T., Kenck, A.R., Key, C.F., Miller, C.J., Specht, T.D., 1989. Final report of the third exploration phase, Marajó. Belém: Texaco/Canada. Report 61 p.

Cordani, U.G., Sato, K., Teixeira, W., Tassinari, C.C.G., Basei, M.A.S., 2000. Crustal evolution of the South American platform. In: Cordani, U.G., Milani, E.J., Thomaz Filho, A., Campos, D.A. (Eds.), 31 International Geological Congress on Tectonic Evolution of South America, Rio de Janeiro, pp. 19–40.

Costa, M.L., Moraes, E.L., 1992. As grandes reservas de caulim e a lateritização na Amazônia. In: 37 Congresso Brasileiro de Geologia, SBG, São Paulo. Boletim de Resumos Expandidos 1, pp. 588–589.

Costa, M.L., Moraes, E.L., 1998. In: Mineralogy, geochemistry and genesis of kaolins from the Amazon regionMineralium Deposita, Vol. 33. Spring-Verlag, pp. 283–297.

Costa, J.B.S., Hasui, Y., Bemerguy, R.L., Soares Jr., A.V., Villegas, J.M.C., 2002. Tectonics and paleogeography of the Marajó Basin, northern Brazil. Anais da Academia Brasileira de Ciências 74 (3), 519–531.

CPRM, 2002. Serviço Geológico do Brasil. Geologia, tectônica, Recursos Minerais do Brasil. Sistema de Informações Geográficas (SIG). http://wwwa.geoambiente.com.br/website/cprm1/viewer.htm.

Francisco, B.H.R., Lowenstein, P., Silva, O.F., Silva, G.G., 1971. Contribuição à Geologia da Folha de São Luís (SA-23) no Estado do Pará. Boletim Museu Paraense Emílio Goeldi, Belém, Série Geologia 17, 1–40.

Galvão, M.V.G., 1991. Evolucão Termodinâmica da Bacia do Marajó, Estado do Pará, Brasil. 193 p. (MSc Dissertation., Departamento de Geologia, Universidade Federal de Ouro Preto, Ouro Preto).

Gaudette, H.E., Lafon, J.M., Macambira, M.J.B., Moura, C.A.V., Scheller, T., 1998. Comparison of single filament Pb evaporation/ionization zircon ages with conventional U–Pb results: examples from Precambrian of Brazil. Journal of South American Earth Science 11, 351–363.

Hurley, P.M., Almeida, F.F.M., Melcher, G.C., Cordani, V.G., Rand, J.R., Kawashita, K., Vandoros, P., Pinson, W.H., Fairbairn, H.W.,

1967. Test of drift by comparison of radiometric ages. Science 157, 495–500.

Hurst, V.J., Bosio, N.J., 1975. Rio Capim Kaolin deposits, Brazil. Economic Geology 70 (5), 990–992.

Klein, E.L., Moura, C.A.V., 2001a. Age constraints on granitoids and metavolcanic rocks of the São Luís Craton and Gurupi Belt, Northern Brazil: implications for lithoestratigraphy and geological evolution. International Geology Review 43, 237–253.

Klein, E.L., Moura, C.A.V., 2001b. Síntese geológica e geocronológica do Cráton São Luís e Cinturão Gurupi: implicações para a litoestratigrafia e modelos geotectônicos. In: 7 Simpósio de Geologia da Amazônia, SBG, Belém, Resumos Expandidos (CD-ROM).

Klein, E.L., Moura, C.A.V., 2003. Síntese Geológica e Geocronológica do Cráton São Luís e do Cinturão Gurupi na Região do Rio Gurupi (NE-Pará/NW-Maranhão). Revista do Instituto de Geociências USP Série Científica 3, 97–112.

Kober, B., 1986. Whole-grain evaporation for $^{207}Pb/^{206}Pb$-age-investigations on single zircons using a double-filament thermal ion source. Contribution Mineralogy and Petrology 93, 482–490.

Kober, B., 1987. Single grain evaporation combined with Pb emitter bedding $^{207}Pb/^{206}Pb$ investigations using thermal ion mass spectrometry and implications to zirconology. Contribution Mineralogy and Petrology 96, 63–71.

Kotschoubey, B., Truckenbrodt, W., Hieronymus, B., 1996. Depósitos de caulim e argila semi-flint no nordeste do Estado do Pará. Revista Brasileira de Geociências 26 (2), 71–80.

Krebs, A.S.J., Arantes, J.I., 1973. Pesquisa de caulim no Rio Capim, Estado do Pará. ln: Anais 27 Congresso Brasileiro de Geologia, SBG, Aracaju 1, 181–191.

Leite, J.A.D., Saes, G.S., 2003. Geocronologia Pb/Pb de Zircões Detríticos e Análise Estratigráfica das Coberturas Sedimentares Proterozóicas do Sudoeste do Cráton Amazônico. Revista do Instituto de Geociências USP Série Científica 3, 113–127.

Macambira, M.J.B., Lafon, J.M., 1995. Geocronologia da Província Mineral de Carajás; síntese dos dados e novos desafios. Boletim Museu Paraense Emílio Goeldi, Belém, Série Ciências da Terra 7, 263–288.

Machado, N., Lindenmayer, Z., Krogh, T.E., Lindenmayer, D., 1991. U–Pb geochronology of archaean magmatism and basement reactivation in the Carajás area, Amazon shield, Brazil. Precambrian Research 49, 329–354.

Machado, N., Lindenmayer, D., Lindenmayer, Z., 1988. Geocronologia U–Pb da Província Metalogenética de Carajás, Pará: resultados preliminares. In: 7 Anais Congresso Latinoamericano de Geologia, SBG/DNPM, pp. 339–347.

Monteiro, R.W., 1977. Elementos traços no caulim do Rio Capim, estado do Pará. Belém. 66 p. (MSc Dissertation, Centro de Geociências, Universidade Federal do Pará).

Moraes, E.L., 1994. Estudo mineralógico, geoquímico e físico de caulins em São Gabriel da Cachoeira – AM, Manaus-Itacoatiara – AM e BR-010 / Rio Capim – PA (Amazônia). 130 p. (MSc Dissertation, Centro de Geociências, Universidade Federal do Pará).

Moraes, E.L., Costa, M.L., 1993. Correlações físicas, mineralógicas e geoquímicas entre caulins derivados de gnaisses e rochas sedimentares na Amazônia Ocidental. In: IV Congresso Brasileiro de Geoquímica, SBG, Brasília, Resumos Expandidos, pp. 215–217.

Moura, C.A.V., Abreu, F.A.M., Klein, E.L., Palheta, E.S.M., Pinheiro, B.L.S., 2003. Geochronology of the São Luis Craton and the Gurupi Belt, Brazil. In: South American Symposium on Isotope Geology, SSAGI, Salvador. Short Papers 4, pp. 225–228.

Moura, C.A.V., Gaudette, H.E., 1993. Zircons ages of the basement orthogneisses of the Araguaia Belt, north-cental Brazil. In: Anais 4 Congresso Brasileiro de Geoquímica, SBGq, Brasília, pp. 232–235.

Murray, H.H., Partridge, P., 1981. Genesis of Rio Jari Kaolin. International Clay Conference. Development in Sedimentology 35, 279–291.

Nascimento, M.S., 2002. Minerais pesados em depósitos cretáceos e terciários do leste da Sub-Bacia de Cametá, NE do Pará. 99 p. (MSc Dissertation, Centro de Geociências, Universidade Federal do Pará).

Palheta, E.S.M., 2001. Evolução geológica da região nordeste do Estado do Pará com base em estudos estruturais e isotópicos de granitóides. 144 p. (MSc Dissertation, Centro de Geociências, Universidade Federal do Pará).

Rino, S., Komiya, T., Brian, F.W., Katayama, I., Motoki, A., Hirata, T., 2004. Major episodic increases of continental crustal growth determined from zircon ages of river sands; implications for mantle overturns in the Early Precambrian. Physics of the Earth and Planetary Interiors 146, 369–394.

Santos Jr., A.E., Rossetti, D.F., 2003. Paleoambiente e estratigrafia da Formação Ipixuna, área do Rio Capim, leste da Sub-Bacia de Cametá. Revista Brasileira de Geociências 33 (3), 313–324.

Santos Jr., A.E., 2002. Reconstrução Paleoambiental e estratigráfica de depósitos cretáceos e terciários expostos na Sub-Bacia de Cametá, Norte do Brasil. 131 p. (MSc Dissertation, Centro de Geociências, Universidade Federal do Pará).

Sousa, D.J.L., 2000. Caracterização geológica, mineralógica, química e física do caulim da mina da RCC – Rio Capim Caulim (PA). 119 p. (MSc Dissertation, Centro de Geociências, Universidade Federal do Pará).

Sousa, D.J.L., Angélica, R.S., Costa, M.L., Mangolg, K.A., 1999. A relação da lateritização com o depósito de caulim da mina RCC – Rio Capim Caulim, NE do Estado do Pará. In: Anais 7 Congresso Brasileiro de Geoquímica, SBGq, Salvador, pp. 418–420.

Sousa, D.J.L., Varajão, A.F.D.C., Scheller, T., 2002. A possível proveniência dos zircões do caulim da mina da Imerys Rio Capim Caulim – NE do Pará. In: 41 Congresso Brasileiro de Geologia SBG-NE, João Pessoa, Paraíba 1, p. 511.

Stacey, J.S., Kramers, J.D., 1975. Approximation of terrestrial lead isotope evolution by a two stage model. Earth and Planetary Science Letters 26, 207–221.

Tassinari, C.C.G., Bittencourt, J.S., Geraldes, M.C., Macambira, M.J.B., Lafon, J.M., 2000. The Amazonian Craton. In: Cordani, U.G., Milani, E.J., Thomaz Filho, A., Campos, D.A. (Eds.), 31st International Geological Congress on Tectonic Evolution of South America, Rio de Janeiro, pp. 41–95.

Tassinari, C.C.G., Macambira, M.J.B., 1999. Geochronological provinces of the Amazonian Craton. Episodes 22, 174–182.

Teixeira, N.P., Bettencourt, J.S., Moura, C.A.V., Dall'Agnol, R., Macambira, E.M.B., 2002. Archean crustal sources for Paleoproterozoic tin-mineralized granites in the Carajás Province, SSE Pará, Brazil: Pb/Pb geochronology and Nd isotope geochemistry. Precambrian Research 119, 257–275.

Teixeira, W., Tassinari, C.C.G., Cordani, U.G., Kawashita, K., 1989. A review of the geochronology of the Amazonian Craton: tectonic implications. Precambrian Research 42, 213–227.

Villas, R.N.N., 1982. Geocronologia das intrusões ígneas na bacia do rio Guamá, nordeste do Estado do Pará. In: Anais 2 Simpósio de Geologia da Amazônia, SBG, Belém, 1, pp. 233–247.

Villegas, J.M.C., 1994. Geologia Estrutural da Bacia do Marajó. 119 p. (MSc Dissertation, Centro de Geociências, Universidade Federal do Pará).

Wanderley Filho, J.R. 1980. Geologia do Granitóide Mirasselvas, Nordeste do Pará. In: Anais 31 Congresso Brasileiro Geologia, SBG, Camboriú, 2, p. 426.